Discovery of thiazolo[5,4-c]isoquinoline based compounds as acetylcholinesterase inhibitors through computational target prediction, molecular docking and bioassay

Letícia D. Costa [a], Carlos F.M. Silva [a,*], Diana C.G.A. Pinto [a], Artur M.S. Silva [a], Florbela Pereira [b,*], Maria Amparo F. Faustino [a], Augusto C. Tomé [a,*]

[a] LAQV-REQUIMTE, Department of Chemistry, University of Aveiro, 3810-193 Aveiro, Portugal
[b] LAQV-REQUIMTE, Department of Chemistry, NOVA School of Science and Technology, NOVA University of Lisbon, Caparica 2829-516, Portugal

ARTICLE INFO

ABSTRACT

A computer-aided drug design (CADD) approach was developed for a focused chemical library comprising a series of sixteen thiazolo[5,4-c]isoquinoline derivatives. Little is known about this group of heteroaromatic compounds, both from the point of view of their synthesis and their biological properties. First, our CADD approach included target prediction by Mondrian conformal prediction with the ChEMBL database. The acetylcholinesterase (AChE) was identified as having a high probability of thiazolo[5,4-c]isoquinolines being active against it. Secondly, the molecular docking predictions revealed four promising thiazoloisoquinolines (2, 7, 13 and 14) according to their prominent ligand-protein energy scores and relevant binding affinities with the AChE pocket residues. The subsequent *in vitro* evaluation of promising hits and related ones revealed a set of novel AChE inhibitors. Therefore, the findings reported herein may provide a new strategy for discovering novel AChE inhibitors.

1. Introduction

Alzheimer's disease (AD), a progressive neurodegenerative disorder, is the most common type of dementia. AD is characterized by the deficit of acetylcholine in the cholinergic system and the deposition of β-amyloid (Aβ) in the form of neurofibrillary tangles and amyloid plaques [1]. Over 55 million people worldwide lived with dementia in 2020 [2], and this number will substantially increase in the near future. It will almost double every 20 years, reaching 78 million in 2030 and 139 million in 2050 [2]. The cholinergic system plays an important role in regulating learning and memory processes, and it has been targeted for the design of drugs to treat AD. Cholinesterase inhibitors directly enhance cholinergic transmission by inhibiting AChE, which hydrolyses acetylcholine [1]. Thus, the discovery of new compounds that may be AChE inhibitors continues to be a topic of great interest, here we highlight some works that successfully explore the synthesis of new organic compounds such as halogen-containing chalcones [3] or Zn(II), Ga(III) or In(III) complexes of tetra-substituted phthalocyanines [4] and benzimidazole-functionalized Pd-based complexes [5] as AChE

inhibitors. Several AChE structures have been deposited in the Protein Data Bank (PDB) with different active binding sites. It is worth to refer that the binding site of human AChE is significantly different from that of *Torpedo* AChE, leading, for instance, to the binding of donepezil (a second FDA-approved anti-Alzheimer's drug). Cheung et al. reported the high-resolution crystal structures of human AChE alone (PDB ID 4EY4) and in complexes with drug ligands such as donepezil (PDB ID 4EY7) [6]. The authors concluded that the human AChE is a better starting model than the *Torpedo* enzyme for structure-based drug design, modeling, docking, and molecular dynamics computations [6]. The human AChE active site is a long gorge with a total length of approximately 20 Å [7] (Fig. 1), consisting mainly of an active catalytic site (CAS) at the bottom of the gorge (His447, Ser203, Trp86). In contrast, the peripheral anionic site (PAS) is near the gorge's entrance (Trp286, Tyr 72, Tyr341). A narrow groove connects these two sites (Tyr124 and Phe295). Compounds interacting with CAS and PAS are desirable, as they are thought to exert multiple therapeutic effects [7,8], as seen with donepezil.

Thiazoloisoquinolines are a group of heteroaromatic compounds that

---

* Corresponding authors.
E-mail addresses: silva.c@ua.pt (C.F.M. Silva), florbela.pereira@fct.unl.pt (F. Pereira), actome@ua.pt (A.C. Tomé).

have been little explored from a synthesis standpoint and in terms of their applications [9]. A probable reason for this is the lack of simple routes for their synthesis, *e.g.* the access to the [5,4-*c*] isomer requires a multi-step procedure from 4-aminoisoquinoline or 4-acetylamino-1--phenyl-1,4-dihydro-3(2*H*)-isoquinolinone [9,10]. Tomé and coworkers recently reported a new and straightforward method for synthesizing thiazolo[5,4-*c*]isoquinolines from the reaction of dithiooxamide with 2-halobenzaldehydes [9]. So far, only thiazolo[5,4-*c*]isoquinolin-5 (4*H*)-ones and their *O*-alkyl derivatives have found application in the medicinal field, namely as anti-inflammatory and anti-anxiety agents [11]. There are a few examples of drugs approved by regulatory agencies to treat AD as reversible AChE inhibitors, namely: donepezil (i), tacrine (ii), rivastigmine (iii) and galantamine (iv), as well as huperzine A (v) in clinical trials (Fig. 2). All these AChE inhibitors, except for rivastigmine (iii), have a heterocyclic nitrogen ring in their chemical structure, as highlighted in blue in Fig. 2. The isoquinoline scaffold in the library of compounds studied in this work allowed for exploring a new chemical space of thiazoloisoquinolines in AChE inhibition, highlighted in blue in the template (1) of Fig. 2.

In the past decades, computer-aided drug design (CADD) methods have become invaluable tools in developing therapeutically important small molecules, and higher hit rates than those obtained through high throughput screening (HTS) approaches alone have been observed [12–14]. The relevance of CADD methods in drug discovery was recently highlighted by Gasteiger [15], who states "*...all drugs developed in recent years have benefited from the use of chemoinformatics methods in one way or another.*"

Herein, a CADD approach was developed for a focused chemical library comprising a series of thiazolo[5,4-*c*]isoquinolines synthesized by the dithiooxamide/2-halobenzaldehyde protocol. First, our CADD approach included target prediction by Mondrian conformal prediction with the ChEMBL database, which comprises data from 550 human protein targets with different bioactivity profiles, and a high probability of thiazolo[5,4-*c*]isoquinolines being active against AChE was identified. Secondly, the molecular docking predictions revealed four

promising thiazoloisoquinolines (2, 7, 13 and 14) according to their prominent ligand–protein energy scores and relevant binding affinities with the AChE pocket residues. The subsequent *in vitro* evaluation of promising hits and related ones confirmed docking predictions for one derivative (14) and revealed a set of three derivatives (1, 6 and 15) as novel AChE inhibitors, all with an $IC_{50} \leq 10$ μM against AChE. AChE inhibition by kinetic analysis of the most promising derivatives (6 and 14) shows a mixed-type inhibitory behavior for both derivatives, which aligns with the inhibitory behavior reported for donepezil.

2. Results and discussion

2.1. In silico target prediction

A focused library of sixteen thiazolo[5,4-*c*]isoquinolines (Fig. 3) was used in this study. The synthesis and structural characterization of these compounds was already reported. [9] The template (no substituted derivative, 1) was synthesized by a transformation of compound 4 using our methodology. NMR and MS established the structure of this compound (see Supplementary data).

The target prediction was performed using the Mondrian conformal prediction (MCP) [16] and the ChEMBL database [17]. In total, the ChEMBL database (release 24) contains more than 15 million bioactivity measurements for 1.8 million distinct compounds [17]. The prediction for unsubstituted thiazolo[5,4-*c*]isoquinoline 1 (Fig. 3) was performed, and the AChE enzyme was identified as a possible target. The Tanimoto coefficient (TC) of similarity between 1 and each one of the fifteen thiazolo[5,4-*c*]isoquinolines (2–16) was calculated, and TC values for all derivatives were in the range of 0.69–0.88.

2.2. Molecular docking against AChE

Molecular docking, using the Autodock Vina software, was applied to elucidate the binding action of sixteen thiazolo[5,4-c]isoquinolines (1-16) against AChE (PDB ID 4EY4) [6]; the thiazolo[5,4-*c*]isoquinoline 1

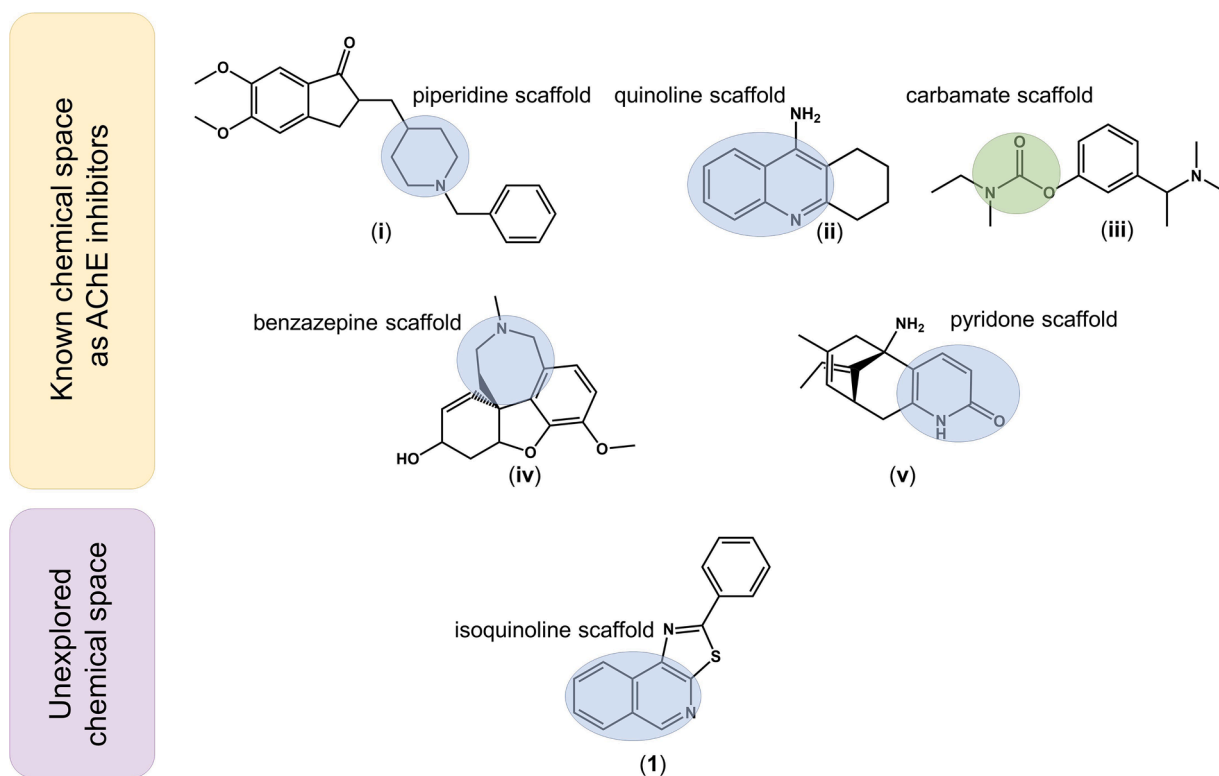**Fig. 1.** Representation of CAS and PAS in the AChE [7].

Fig. 2. Chemical structures of the known AChE inhibitors: donepezil (i), tacrine (ii), rivastigmine (iii), galantamine (iv) and huperzine A (v). Chemical structure of the template (1) used in this study.

#	R^1	R^2	R^3	R^4	R^5/R^9	R^6/R^8	R^7
Template (1)	H	H	H	H	H/H	H/H	H
2	F	F	F	F	F/F	F/F	F
3	H	H	H	H	F/H	H/H	H
4	H	H	H	H	Cl/H	H/H	H
5	H	H	H	F	F/H	F/H	H
6	F	H	H	H	F/F	H/H	H
7	H	H	H	Cl	Cl/H	Cl/H	H
8	H	H	Cl	H	H/Cl	H/H	Cl
9	Cl	H	H	H	Cl/Cl	H/H	H
10	Br	H	H	H	Br/Br	H/H	H
11	Cl	Cl	H	H	Cl/Cl	Cl/H	H
12	Cl	H	H	Cl	Cl/Cl	H/Cl	H
13	F	F	H	F	F/F	F/F	H
14	CF_3	H	H	H	F/CF_3	H/H	H
15	CH_3	H	H	H	Cl/CH_3	H/H	H
16	H	H	H	H	NO_2/H	H/H	H

Fig. 3. Thiazolo[5,4-*c*]isoquinolines used in this study.

(no substituents), five fluoro-substituted derivatives (2, 3, 5, 6 and 13), seven chloro-substituted derivatives (4, 7, 8, 9, 11, 12 and 15), one bromo-substituted derivative (10), one trifluoromethyl-substituted derivative (14) and one nitro-substituted derivative (16), as shown in Fig. 3. The results of molecular docking on the AChE for the studied thiazolo[5,4-*c*]isoquinolines are shown in Table 1. In this study, two

positive controls, donepezil and tacrine, both AChE inhibitors used for the therapy of Alzheimer's disease, were included.

The derivatives with the lowest ΔG_B calculated, *i.e.,* the most promising thiazolo[5,4-*c*]isoquinolines according to the docking studies, are 14 (trifluoromethyl-substituted), 2 (fluoro-substituted), 13 (fluoro-substituted) and 7 (chloro-substituted) with values of −11.0,

Table 1

Calculated free binding energies (ΔG_B, in kcal/mol) and the detailed interactions established upon docking the sixteen thiazolo[5,4-*c*]isoquinolines, donepezil and tacrine against AChE.

Compound	Substituent	ΔG_B (kcal/mol)	H-bond residues	Hydrophobic interaction residues
1	hydrogen	–9.4	—	Tyr72[2], Trp286[2], Tyr341[2], Tyr124, Tyr337[1], Phe338, Val294, Phe295
2	fluoro	–10.9	Phe295	Trp286[2], Glu292, Tyr124, Tyr341[2]
3	fluoro	–9.5	Tyr337[1]	Trp286[2], Phe295, Val294, Tyr341[2], Phe297, Gly122, Phe338, Ser203[1], His447[1], Gly121, Tyr124
4	chloro	–9.6	Tyr337[1]	Trp286[2], Phe295, Val294, Tyr341[2], Phe297, Gly122, Phe338, Ser203[1], His447[1], Gly121, Tyr124
5	fluoro	–9.7	—	Glu292, Ser293, Trp286[2], Asp74, Tyr124, Phe338, Tyr341[2]
6	fluoro	–9.4	—	Glu292, Ser293, Phe295, Phe338, Tyr124, Tyr341[2], Trp286[2]
7	chloro	–10.1	—	Trp286[2], Tyr124, Try337[1], Phe338, Phe295, Tyr341[2], Val294, Ser293
8	chloro	–9.3	—	Trp286[2], Tyr72[2], Asp74, Tyr341[2], Tyr124
9	chloro	–8.9	—	Glu292, Trp286[2], Tyr341[2], Ser293, Val294, Phe295
10	bromo	–8.5	—	Gln291, Glu292, Leu289, Trp286[2], Tyr124, Tyr341[2]
11	chloro	–9.3	—	Trp286[2], Leu289, Asp74, Tyr341[2], Tyr124
12	chloro	–9.1	Ser293	Tyr341[2], Val294, Trp286[2], Try124, Asp74
13	fluoro	–10.4	—	Glu292, Trp286[2], Phe295, Tyr341[2]
14	trifluoromethyl	–11.0	Phe295, Tyr337[1]	Tyr341[2], Asp74, Trp286[2], Tyr124, Phe338, Phe297, Gly122, His447[1], Gly121, Ser203[1]
15	chloro	–9.2	—	Glu292, Leu289, Ser293, Trp286[2], Val294, Phe295, Tyr341[2], Tyr124
16	nitro	–8.7	—	Phe295, Tyr341[2], Tyr124, Trp286[2], Leu289, Gln291, Glu292
donepezil[3]	—	–9.2	—	Trp286[2], Try72[2], Tyr341[2], Phe338, Phe297, Tyr124, Gly122, Tyr337[1]
tacrine[3]	—	–8.8	—	Trp286[2], Try72[2], Phe295, Tyr341[2], Phe338, Tyr124

[1] CAS amino acid residues.
[2] PAS amino acid residues.
[3] Positive Control.

–10.9, –10.4 and –10.1 kcal/mol, respectively (Table 1). It is also important to note that donepezil and tacrine, known anti-Alzheimer's agents, have ΔG_B values of –9.2 kcal/mol and –8.8 kcal/mol, respectively. As mentioned above, there appears to be a therapeutic advantage of compounds that interact simultaneously with the CAS and PAS amino acid residues of the AChE, as is the case with control donepezil. In this way, we have the following thiazolo[5,4-*c*]isoquinolines that interact simultaneously with the CAS and PAS sites: 14 (trifluoromethyl-substituted), 4 (chloro-substituted), 3 (fluoro-substituted), and the unsubstituted derivative 1 with values of –11.0, –9.6, –9.5 and –9.4 kcal/mol, respectively (Table 1).

In Fig. 4, the best-docked poses for the most probable lead-like anti-Alzheimer's AChE inhibitor 14 (Fig. 2) and for the control donepezil were shown.

2.3. In vitro AChE and butyrylcholinesterase (BuChE) inhibitory activity

The AChE and BuChE inhibitory activity of the theoretically identified most promising derivatives (14 and 2), as well as some less promising ones that are interesting for a Structure–Activity Relationship (SAR) analysis (1, 6, 9, 10, 11, 12 and 15), were evaluated against *Electrophorus electricus* AChE (eeAChE) and *equine serum* BuChE following an adaptation of the Ellman's method [18]. It is important to emphasize that (11 + 12) represents a 1:1 mixture of two isomers whose separation by preparative TLC was unsuccessful due to their similar R_f values. Thus, the biological activity described here reflects the contribution of both compounds. Both eeAChE and *equine serum* BuChE are excellent models for evaluating the cholinesterases (ChEs) inhibitory activity, as these enzymes display extensive sequence identity with the human enzymes [19]. The obtained results from these *in vitro* assays are represented in Table 2, with donepezil used as the positive control.

From the results in Table 2, the potential of thiazolo[5,4-*c*]iso-quinoline derivatives as selective AChE inhibitors appears clear, with five of the evaluated derivatives presenting IC_{50} values below 10 μM against AChE, corroborating the theoretical studies. Furthermore, the results demonstrated that, with the exception of derivative 2, the fluorinated derivatives (6 and 14) are the most active from this series of compounds. When compared with the unsubstituted thiazolo[5,4-*c*]isoquinoline 1, the insertion of fluoro atoms increases the inhibitory activity. Compound 6 was the most active against AChE (IC_{50} = 4.74 ± 0.74 μM). No inhibitory activity was observed against BuChE by any thiazolo[5,4-*c*]isoquinoline.

2.4. Kinetic analysis of AChE inhibition

The mechanism of the AChE inhibition by compounds 6 and 14 was evaluated through Lineweaver–Burk plot analysis (Fig. 5). The Lineweaver–Burk plots against AChE demonstrate that, for derivatives 6 and 14, the slopes increase compared to the absence of inhibitor, corresponding to a decrease of V_{max}. Furthermore, these Lineweaver–Burk plots also show an increase in the interception to the x-axis (1/[S] axis), demonstrating that the K_m values decrease in the presence of these two inhibitors (6 and 14). This information indicates a mixed-type inhibitory behaviour for both compounds, suggesting that these inhibitors might bind to the free enzyme and the enzyme-substrate complex. Considering the decrease in the K_m values, it is possible to assume that these inhibitors favour binding to the enzyme-substrate complex. A similar mixed-type inhibitory behaviour has been well established and described for donepezil by kinetic measurements [6]. However, contrary to what seems to happen with the thiazolo[5,4-*c*]isoquinoline derivatives (6 and 14), donepezil binds with greater stability to the substrate-free enzyme than to the substrate-loaded enzyme, taking into account kinetic studies, molecular dynamics simulations and docking and free energy calculations [20].

2.5. Structure–Activity Relationship (SAR) studies

To compare the structural similarity between thiazolo[5,4-*c*]iso-quinolines (1–16), and the known inhibitors of the AChE, donepezil and tacrine, the Tanimoto similarity score (TSS) between them was determined. The TSS values obtained between the derivatives and donepezil are in the range of 0.445 and 0.52. For tacrine, the TSS values range from
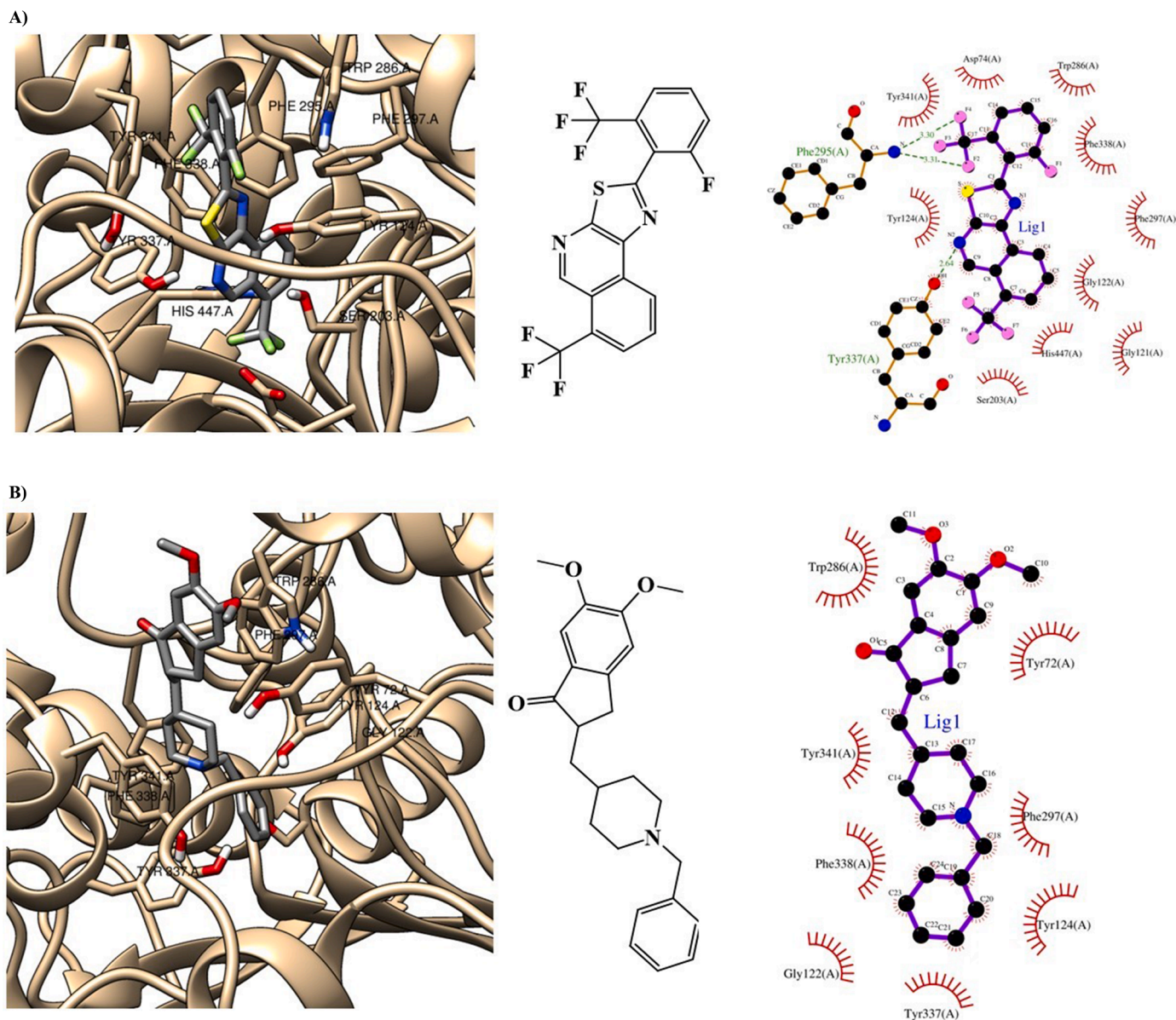
A)

B)

Fig. 4. Interaction profiles of the best-docked poses for the A) thiazolo[5,4-*c*]isoquinoline 14 and B) donepezil.

0.406 and 0.466. There is a clear correlation between the highest TSS values and the most promising inhibitors of AChE, in accordance with their estimated binding scores (Table 1) and IC$_{50}$ obtained against eeAChE (Table 2) for the inhibitor donepezil. For example, the most active derivative, compound 6 (Table 2), has one of the highest TSS values with the inhibitor donepezil of 0.477 and, also has one of the lowest estimated binding energies against AChE (–9.4 kcal/mol, Table 1). On the other hand, the derivative 10 has the same substitution pattern as 6, but with the fluoro atoms replaced by bromo atoms (see Fig. 2). For derivative 10, one of the lowest TSS with donepezil (0.461), one of the highest estimated binding energies against AChE (–8.5 kcal/mol, Table 1) and one of the highest IC$_{50}$ values against eeAChE (10.32 mM, Table 2) were obtained. ChemAxon's 3D alignment tool aligned the extended atom types of 6 and 10 derivatives and the control donepezil, as shown in Fig. 6.

With the exception of derivative 2, the fluoro-substituted derivatives (6, 14) that were experimentally evaluated showed inhibitory activity, presenting IC$_{50}$ values below 10 μM against AChE (Table 2). Conversely, only one of the compounds substituted with chloro or bromo atoms has an IC$_{50}$ lower than 10 μM (15, Table 2), the remaining ones (2, 9, 10 and

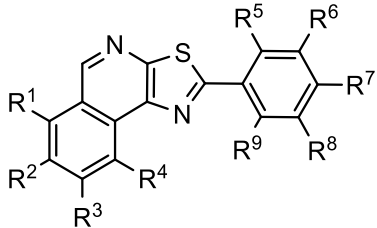11 + 12, Table 2) have an IC$_{50}$ higher than 10 μM against AChE. The presence of fluoro atoms in the thiazolo[5,4-*c*]isoquinolines appears advantageous for improving the activity against AChE. That is evident by comparing the results of derivatives 6 (bearing F atoms) and 10 (bearing Br atoms), or the results of derivatives 14 (bearing a -CF$_3$ group) and 15 (bearing a -CH$_3$ group).

3. Conclusions

The results suggest that the CADD approach, relying on a structure-based methodology supported by a preliminary experimental evaluation, could predict new AChE inhibitors from a focused chemical library comprising a series of thiazolo[5,4-*c*]isoquinolines. In this way, lead compounds for developing new drugs with the potential for treating Alzheimer's disease can be identified and proposed. Although the thiazolo[5,4-*c*]isoquinoline derivative 6 is far from being studied on its interaction with AChE or AChE-substrate complex, it can be assumed that it has the potential to be studied as an AChE inhibitor, as we see that its behavior is very similar to donepezil. Further studies would help to understand the extent of the effect of the thiazolo[5,4-*c*]isoquinoline

Table 2
ChE inhibitory activity of selected thiazolo[5,4-*c*]isoquinolines and donepezil.

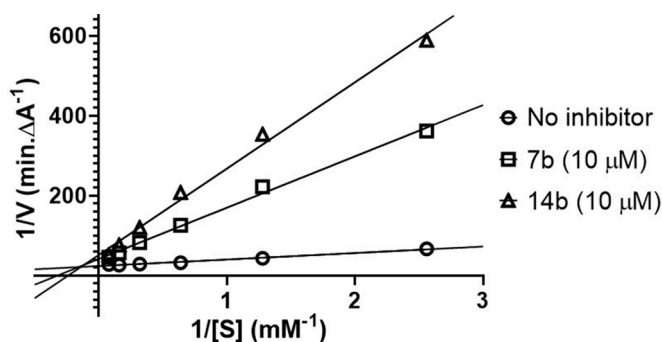| Compound	R groups									eeAChE [IC$_{50}$ (μM)]	BuChE [IC$_{50}$ (μM)]
	R^1	R^2	R^3	R^4	R^5	R^6	R^7	R^8	R^9		
1	H	H	H	H	H	H	H	H	H	8.44 ± 0.77	>20
2	F	F	F	F	F	F	F	F	F	16.34 ± 3.14	>20
6	F	H	H	H	F	H	H	H	F	4.74 ± 0.21	>20
9	Cl	H	H	H	Cl	H	H	H	Cl	11.22 ± 1.48	>20
10	Br	H	H	H	Br	H	H	H	Br	10.32 ± 1.81	>20
11 + 12	Cl	Cl (11), H (12)	H	H (11), Cl (12)	Cl	Cl	H	H	Cl	12.90 ± 1.25	>20
14	CF$_3$	H	H	H	F	H	H	H	CF$_3$	8.23 ± 1.23	>20
15	CH$_3$	H	H	H	Cl	H	H	H	CH$_3$	7.05 ± 0.81	>20
Donepezil										0.025 ± 0.005	4.72 ± 0.95

Fig. 5. Lineweaver–Burk plots resulting from the subvelocity curve of the AChE activity with different substrate concentrations (0.39–12.5 mM) in the absence of inhibitor and in the presence of 6 (10 μM) and 14 (10 μM).

scaffold on AChE-ligand interactions and, in particular, where the molecule centers its action.

4. Methods

4.1. Target prediction by Mondrian conformal prediction (MCP)

The ready to use Mondrian conformal prediction (MCP) models for target prediction provided by ChEMBL team, which can be obtained as a docker image through the following link: "docker run -p 8080:8080 chembl/mcp", were used to predict targets for the derivative 1 (Fig. 2). The docker image was accessed through the Docker v20.10.14 [21]. The MCP models developed by Bosc et al. [16] have been re-implemented with LightGBM, a gradient boosting framework that uses tree-based learning algorithms, in Python using Scikit-learn version 0.19 [22] and the conformal prediction framework was developed using the nonconformist package version 2.1.0 [23].

4.2. Molecular docking

The optimization of the 3D structure of the sixteen thiazolo[5,4-*c*] isoquinolines was performed with the Gaussian 09 program [24] using the hybrid method B3LYP and the base set 6-31G(d,p) [25,26]. The software program OpenBabel (version 2.3.1) [27] was used to convert the mol2 files to PDBQT files. PDBQT files were used for docking to AChE enzyme (PDB ID 4EY4) with AutoDock Vina (version 1.1) [28]. Water molecules, ions and ligands were removed from 4EY4 prior to docking

using the AutoDockTools (http://mgltools.scripps.edu/). The search space coordinates were centered at X: -12.903 Y: -39.296 Z: 26.578; with dimensions of X: 40,000 Y: 40,000 Z: 40,000. Ligand tethering of the AchE enzyme was performed by regulating the genetic algorithm (GA) parameters, using 10 runs of the GA criteria. The docking binding poses were visualized with PyMOL Molecular Graphics System, Version 2.0 Schrödinger, LLC, UCSF Chimera, [29] and LigPlot+ v.2.2.5 [30].

4.3. In vitro AchE and BuChE inhibitory activity

The inhibitory activity of the selected compounds towards AchE and BuChE was evaluated spectrophotometrically through a modified 96-well microplate Ellman's method. Solutions of both *Electrophorus electricus* AchE (eeAChE) and *equine serum* BuChE were prepared as 0.025 U/mL in phosphate buffer, at pH 8, from stock solutions of 5.05 U/mL and 7.50 U/mL, respectively. The stock solutions of the selected compounds were prepared in DMSO at concentrations that would allow the performance of the assay with a percentage of DMSO below 1% in the wells. The remaining assay solutions were all prepared in 0.1 M phosphate buffer, at pH 8, and consisted of 0.5 mM 5,5'-dithiobis(2-nitrobenzoic acid) (DTNB), 2.5 mM acetylthiocholine iodide (ATChI), for the inhibition of AchE, and 2.5 mM butyrylthiocholine iodide (BuTChI), for the inhibition of BuChE. The assay began with 5 min incubation at 37 ºC of 50 μL of the test compound (or phosphate buffer at pH 8, *i.e.,* blank samples) and 100 μL of the enzyme (eeAChE or BuChE). After incubation period, 50 μL of ATChI and 50 μL of DTNB were added to each well, thus initiating the enzymatic reaction. The absorbance values were measured at 415 nm, at every 2.5 min, for a total of 15 min, using a microplate reader (Synergy multi-mode reader; BioTek). The absorbance was measured at seven different concentrations of 40.0, 20.0, 10.0, 5.00, 2.50, 1.25 and 0.625 μM, converted into percentage of inhibition and plotted against the used concentration of inhibitor. The IC$_{50}$ values were calculated using GraphPad Prism 8.0.2 (GraphPad Software Inc.). All the reactions were performed at least in triplicate, including donepezil, which was used as a standard inhibitor.

4.4. Kinetic analysis of AChE inhibition

To obtain the inhibition mechanism of the synthesized compounds (6 and 14), a Lineweaver–Burk plot of *1/V* versus *1/[S]* was performed using six different concentrations of substrate (ATChI; 0.39–12.5 mM) and one concentration of each inhibitor (10 μM) through Ellman's method. Phosphate buffer at pH 8 was used as negative control to construct the Lineweaver-Burk plot in the absence of inhibitor. The

6
3D similarity 0.477

donepezil
inhibitor AChE enzyme
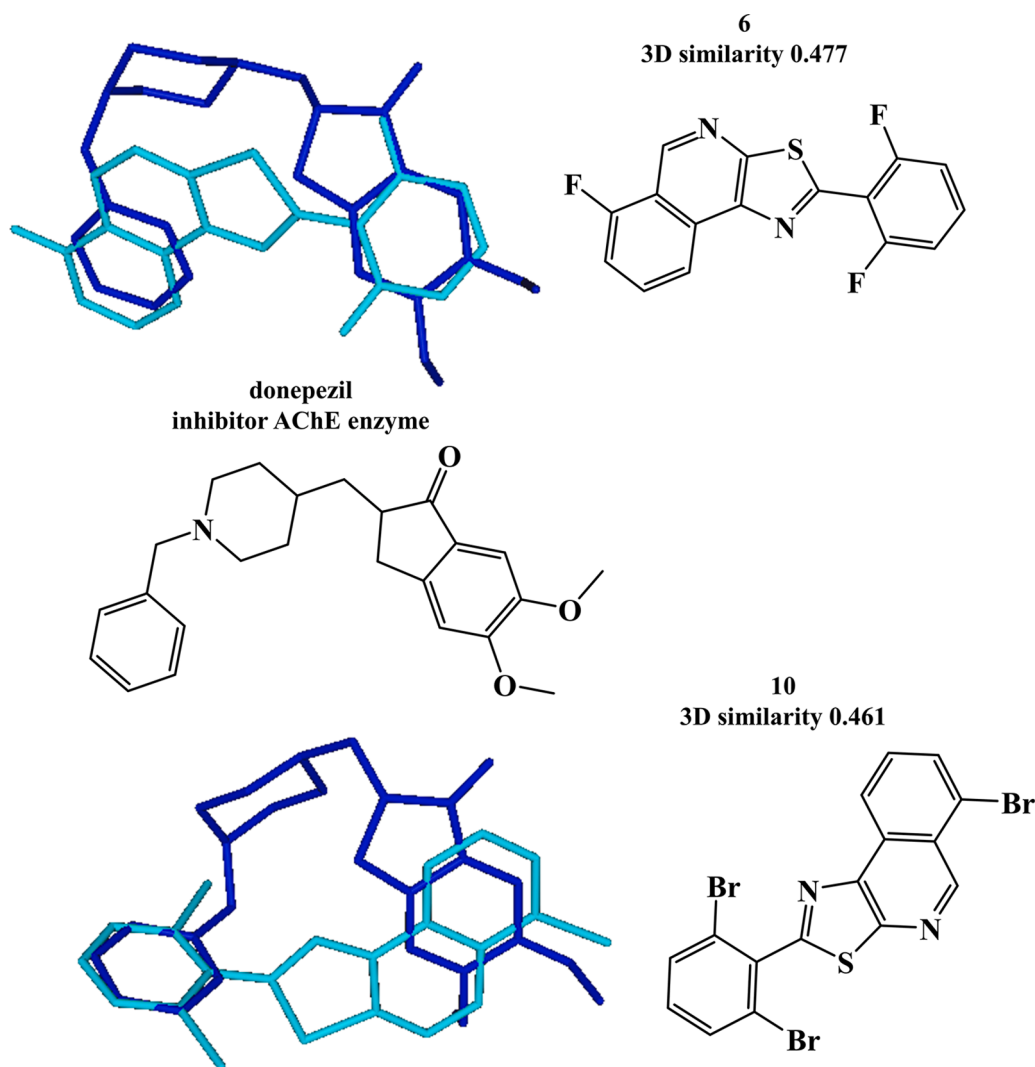
10
3D similarity 0.461

Fig. 6. 3D alignment of derivatives 6 and 10 with donepezil.

experiments were performed at least in triplicate, and data analysis was performed with GraphPad Prism 8.0.2 (GraphPad Software Inc.).

4.5. SAR analysis

ChemAxon's 3D alignment tool version 5.7.13.0 (ChemAxon Ltd., Budapest, Hungary) was used to align thiazolo[5,4-*c*]isoquinolines by extended atom types, with the highest Tanimoto similarity score values and the inhibitors against AChE, donepezil and tacrine.

Associated content

None.

Author contributions

Conceptualization, F.P., M.A.F.F.; synthesis, methodology and investigation, L.D.C, C.F.M.S., F.P.; writing—original draft preparation, L.D.C, F.P. and C.F.M.S.; writing—review and editing, F.P., MA.F.F., A. M.S.S. and A.C.T.; supervision, D.C.G.A.P. and A.C.T.; project administration and funding acquisition, A.C.T. and A.M.S.S.. All authors have read and agreed to the published version of the manuscript.

Declaration of Competing Interest

The authors declare that they have no known competing financial interests or personal relationships that could have appeared to influence the work reported in this paper.

Data availability

No data was used for the research described in the article.

Supplementary materials

Supplementary material associated with this article can be found, in the online version, at doi:10.1016/j.molstruc.2023.136088.

References

[1] P. Anand, B. Singh, A review on cholinesterase inhibitors for Alzheimer's disease, Arch. Pharmacal Res. 36 (2013) 375–399.

[2] International, C. A. S. D. Alzheimer's disease international. https://www.alzint.org/about/dementia-facts-figures/dementia-statistics/, (accessed on 25 July, 2022).

[3] S. Burmaoglu, E.A. Kazancioglu, R. Kaya, M. Kazancioglu, M. Karaman, O. Algul, I. Gulcin, Synthesis of novel organohalogen chalcone derivatives and screening of their molecular docking study and some enzymes inhibition effects, J. Mol. Struct. 1208 (2020) 127868.

[4] A. Gunsel, A.T. Bilgicli, B. Barut, P. Taslimi, A. Ozel, Z. Biyiklioglu, M.N. Yarasir, I. Gulcin, Synthesis of water soluble tetra-substituted phthalocyanines: Investigation of DNA cleavage, cytotoxic effects and metabolic enzymes inhibition, J. Mol. Struct. (2020) 1214.

[5] Y.Gok Dasgin, D.B. Celepci, P. Taslimi, M. Izmirli, A. Aktas, I. Gulcin, Synthesis, characterization, crystal structure and bioactivity properties of the benzimidazole-functionalized PEPPSI type of Pd(II)NHC complexes, J. Mol. Struct. (2021) 1228.

[6] J. Cheung, M.J. Rudolph, F. Burshteyn, M.S. Cassidy, E.N. Gary, J. Love, M. C. Franklin, J.J. Height, Structures of human acetylcholinesterase in complex with pharmacologically important ligands, J. Med. Chem. 55 (2012) 10282–10286.

[7] A. Asghar, M. Yousuf, G. Fareed, R. Nazir, A. Hassan, A. Maalik, T. Noor, N. Iqbal, L. Rasheed, Synthesis, acetylcholinesterase (AChE) and butyrylcholinesterase (BuChE) activities, and molecular docking studies of a novel compound based on combination of flurbiprofen and isoniazide, RSC Adv. 10 (2020) 19346–19352.

[8] Y. Pourshojaei, A. Abiri, K. Eskandari, Z. Haghighijoo, N. Edraki, A. Asadipour, Phenoxyethyl piperidine/morpholine derivatives as PAS and CAS inhibitors of cholinesterases: insights for future drug design, Sci. Rep. 9 (2019) 19855.

[9] L.D. Costa, S. Guieu, M.D.F. Faustino, A.C. Tome, Straightforward synthesis of thiazolo 5,4-c isoquinolines from dithiooxamide and 2-halobenzaldehydes, New J. Chem. 46 (2022) 3602–3615.

[10] I. Tikk, G. Deak, P. Sohar, J. Tamas, Hydroxyiminoisoquinolin-3(2H)-ones. 9. Synthesis of some oxazolo[5,4-c]-, thiazolo[5,4-c]- and 2,3-dihydro-1H-[1,4] oxazino[2,3-c]isoquinolines, J. Heterocycl. Chem. 25 (1988) 273–277.

[11] Winters, G.; Di Mola, N., Inventors; Gruppo Lepetit SpA, assignee. Pyrazolo(3,4-c) and thiazolo(5,4-c)Isoquinolines, methods for preparing them, these compounds for use as antiinflammatory, CNS-depressant and anti-anxiety agents and pharmaceutical compositions Thereof. European patent EP0005745A1. 1979, May 8.

[12] R. Mueller, E.S. Dawson, J. Meiler, A.L. Rodriguez, B.A. Chauder, B.S. Bates, A. S. Felts, J.P. Lamb, U.N. Menon, S.B. Jadhav, A.S. Kane, C.K. Jones, K.J. Gregory, C.M. Niswender, P.J. Conn, C.M. Olsen, D.G. Winder, K.A. Emmitte, C.W. Lindsley, Discovery of 2-(2-Benzoxazoyl amino)-4-Aryl-5-cyanopyrimidine as negative

allosteric modulators (NAMs) of metabotropic glutamate receptor 5 (mGlu5): from an Artificial Neural Network virtual screen to an *in vivo* tool compound, ChemMedChem (7) (2012) 406–414.

[13] G. Sliwoski, S. Kothiwale, J. Meiler, E.W. Lowe, Computational methods in drug discovery, Pharmacol. Rev 66 (2014) 334–395.

[14] T. Katsila, G.A. Spyroulias, G.P. Patrinos, M.-T. Matsoukas, Computational approaches in target identification and drug discovery, Comput. Struct. Biotechnol. J. 14 (2016) 177–184.

[15] J. Gasteiger, Chemistry in Times of Artificial Intelligence, ChemPhysChem 21 (2020) 2233–2242.

[16] N. Bosc, F. Atkinson, E. Felix, A. Gaulton, A. Hersey, A.R. Leach, Large scale comparison of QSAR and conformal prediction methods and their applications in drug discovery, J. Cheminform. 11 (2019) 4.

[17] D. Mendez, A. Gaulton, A.P. Bento, J. Chambers, M. De Veij, E. Felix, M. P. Magarinos, J.F. Mosquera, P. Mutowo, M. Nowotka, M. Gordillo-Maranon, F. Hunter, L. Junco, G. Mugumbate, M. Rodriguez-Lopez, F. Atkinson, N. Bosc, C. Radoux, A. Segura-Cabrera, A. Hersey, A.R. Leach, ChEMBL: towards direct deposition of bioassay data, Nucleic Acids Res. 47 (2019) D930–D940.

[18] G.L. Ellman, K.D. Courtney, V. Andres, R.M. Featherstone, A new and rapid colorimetric determination of acetylcholinesterase activity, Biochem. Pharmacol. 7 (1961) 88–90.

[19] D. Malafaia, A. Oliveira, P.A. Fernandes, M.J. Ramos, H.M.T. Albuquerque, A.M. S. Silva, Chromeno[3,4-b]xanthones as First-in-Class AChE and Aβ aggregation dual-inhibitors, Int. J. Mol. Sci. 22 (2021) 4145.

[20] M.A. Silva, A.S. Kiametis, W. Treptow, Donepezil inhibits acetylcholinesterase via multiple binding modes at room temperature, J. Chem. Inf. Model. 60 (2020) 3463–3471.

[21] M.D. Docker, lightweight linux containers for consistent development and deployment, Linux J. 239 (2014) 2.

[22] F. Pedregosa, G. Varoquaux, A. Gramfort, V. Michel, B. Thirion, O. Grisel, M. Blondel, P. Prettenhofer, R. Weiss, V. Dubourg, J. Vanderplas, A. Passos, D. Cournapeau, M. Brucher, M. Perrot, E. Duchesnay, Scikit-learn: machine learning in Python, J. Mach. Learn. Res. 12 (2011) 2825–2830.

[23] Nonconformist package. https://github.com/donlnz/nonconformist (accessed on 25 July, 2022).

[24] M.J. Frisch, M.A. Robb, J.R. Cheeseman, G. Scalmani, V. Barone, B. Mennucci, G.A. Petersson, H. Nakatsuji, M. Caricato, X. Li, H.P. Hratchian, A.F. Izmaylov, J. Bloino, G. Zheng, J.L. Sonnenberg, M. Hada, M. Ehara, K. Toyota, R. Fukuda, J. Hasegawa, M. Ishida, T. Nakajima, Y. Honda, O. Kitao, H. Nakai, T. Vreven, J.A.J. Montgomery, J.E. Peralta, F. Ogliaro, M. Bearpark, J.J. Heyd, E. Brothers, K.N. Kudin, V.N. Staroverov, T. Keith, R. Kobayashi, J. Normand, K. Raghavachari, A. Rendell, J.C. Burant, S.S. Iyengar, J. J. Tomasi, M. Cossi, N. Rega, J.M. Millam, M. Klene, J.E. Knox, J.B. Cross, V. Bakken, C. Adamo, J. Jaramillo, R. Gomperts, R.E. Stratmann, O. Yazyev, A.J. Austin, R. Cammi, C. Pomelli, J.W. Ochterski, R.L. Martin, K. Morokuma, V.G. Zakrzewski, G.A. Voth, P. Salvador, J.J. Dannenberg, S. Dapprich, A.D. Daniels, O. Farkas, J.B.J.B. Foresman, J.V. Ortiz, J. Cioslowski, D.J. Fox, Gaussian 09, Revision B.01, 2010.

[25] A.D. Becke, A new mixing of Hartree–Fock and local density-functional theories, J. Chem. Phys. 98 (1993) 1372–1377.

[26] A.D. Becke, Density-functional thermochemistry. III. The role of exact exchange, J. Chem. Phys. 98 (1993) 5648–5652.

[27] N.M. O'Boyle, M. Banck, C.A. James, C. Morley, T. Vandermeersch, G. R. Hutchison, Open Babel: an open chemical toolbox, J. Cheminform. 3 (2011) 33, 2011.

[28] O. Trott, A.J. Olson, Software news and update AutoDock Vina: improving the speed and accuracy of docking with a new scoring function, efficient optimization, and multithreading, J. Comput. Chem. 31 (2010) 455–461.

[29] E.F. Pettersen, T.D. Goddard, C.C. Huang, G.S. Couch, D.M. Greenblatt, E.C. Meng, T.E. Ferrin, UCSF chimera - A visualization system for exploratory research and analysis, J. Comput. Chem. 25 (2004) 1605–1612.

[30] A.C. Wallace, R.A. Laskowski, J.M. Thornton, LIGPLOT: a program to generate schematic diagrams of protein-ligand interactions, Protein Eng. 8 (1995) 127–134.